

# Effectively doubling the magnetic field in spin- $\frac{1}{2}$ -spin-1, HSQC, HDQC, coupled HSQC, and coupled HDQC in solution NMR

S. Chandra Shekar,<sup>1,2,a)</sup> Jonathan M. Backer,<sup>1</sup> and Mark E. Girvin<sup>2</sup>

<sup>1</sup>Department of Molecular Pharmacology, Albert Einstein College of Medicine, Yeshiva University, 1300 Morris Park Avenue, Bronx, New York 10461, USA

<sup>2</sup>Department of Biochemistry, Albert Einstein College of Medicine, Yeshiva University, 1300 Morris Park Avenue, Bronx, New York 10461, USA

(Received 20 December 2007; accepted 13 March 2008; published online 9 May 2008)

Pulse sequences for spin- $\frac{1}{2}$ -spin-1 pair heteronuclear single quantum correlation (HSQC), heteronuclear double quantum correlation (HDQC), and coupled-HSQC, and coupled-HDQC NMR spectroscopies are outlined, and experimental realization for a  $^{13}\text{C}$ - $^2\text{H}$  pair is demonstrated in solution state. In both the coupled versions, conditions for generation of in-phase and antiphase multiplets in either dimension are arrived at. The patterns and the intensity ratios are explained. The double quantum (2Q) experiments confirm doubling of *both* the shift frequency and the splitting due to coupling (to spin  $\frac{1}{2}$ ) of the 2Q coherence emanating from spin 1. The frequency doubling is equivalent to the corresponding single quantum (1Q) coherence at double the magnetic field strength. The coupling doubling, however, is independent of the magnetic field strength and a signature feature of the 2Q coherence. The ramification of the relative relaxation rates of 1Q and 2Q coherences is discussed. © 2008 American Institute of Physics. [DOI: 10.1063/1.2906116]

## I. INTRODUCTION

Recently there has been a surge of interest in heteronuclear  $2d$  correlation NMR spectroscopy involving spin- $\frac{1}{2}$ -spin-1 pairs, especially in solid state,<sup>1-3</sup> powered by pulse sequences akin to heteronuclear multiple quantum correlation (HMQC) which in turn is broadly in the same class of pulse techniques such as heteronuclear single quantum correlation (HSQC).<sup>4</sup>

Much like insensitive nuclei enhanced by polarization transfer (INEPT) (Ref. 5), of which it is built of, the HSQC (Refs. 4-6) pulse sequence serves both as a stand-alone experiment and as a building block in innumerable NMR experiments spanning a wide range of applications. Invented in 1979, close on the heels of the advent of multidimensional NMR spectroscopy<sup>7</sup> (and enjoying much in common with it), both INEPT and HSQC schemes are a regular feature in many  $1d$ - $4d$  NMR pulse sequences (e.g., noesy-HSQC and tocsy-HSQC).<sup>8</sup> The bulk of these sequences and the attendant literature are concerned with spin- $\frac{1}{2}$  nuclei and yet there is an impressive body of work on spin pairs involving spin  $> 1/2$ , notably in the solid phase.<sup>1-3,9-12</sup> Remarkably, even in solution state NMR, Kay and co-workers have excited single and double quantum modes involving simultaneously spin-1 ( $^2\text{H}$ ) and spin- $\frac{1}{2}$  nuclei ( $^{13}\text{C}$  and  $^1\text{H}$ ) in their work on measurement of  $^2\text{H}$  quadrupolar relaxation rates.<sup>13,14</sup>

Below, pulse sequences for spin- $\frac{1}{2}$ -spin-1 pair HSQC, HDQC, coupled-HSQC and coupled-HDQC spectroscopies are outlined along with experimental results for a  $^{13}\text{C}$ - $^2\text{H}$  pair. In both of the coupled versions, the conditions for generation of in-phase and antiphase multiplets in either dimension

are established. Formulas for the patterns and the intensity ratios, which were derived from product operator formalism for the density matrix evolution,<sup>7</sup> are given in a sufficiently general form. These formulas in turn guide in parametrization of the pulse sequences to generate the desired effects in terms of intensity and phase characteristics of the crosspeak multiplet patterns. In both the HDQC and coupled-HDQC experiments, spin-1 double quantum coherences (2QC's) are created and selected prior to the spin-1 evolution period. The 2QC precession frequencies are double that of single quantum coherences (1QC's) in the HSQC experiments. The coupled experiments confirm the generation and frequency labeling of 2Q coherences by exhibiting effectively doubled  $J$  coupling. The frequency doubling in the 2Q experiments leads to doubling of the resolution provided that the relaxation rate for the 2Q coherence is not greater than that for the 1Q coherence. Calculations based on the formulas provided by Millet *et al.*<sup>14</sup> are presented graphically, and indicate that for increasing molecular weight there is a possibility that the relaxation properties of 2Q coherences may be more favorable than those of 1Q coherences.

## II. EXPERIMENTAL

The sample consisted of a mixture of 60% deuterated benzene ( $\text{C}_6\text{D}_6$ ) and 40% dioxane; thus  $^{13}\text{C}$  is present only at natural abundance of 1%. All NMR experiments were carried out at 300 K. All spectra were acquired on a Bruker DRX600 spectrometer operating at 14 T (resulting in Larmor frequencies of 600 MHz for  $^1\text{H}$ , 150 MHz for  $^{13}\text{C}$ , and 92 MHz for  $^2\text{H}$ ). The  $^{13}\text{C}$  pulses were emitted at 125 ppm with a strength of 10 kHz, while  $^2\text{H}$  pulses were emitted at 9.2 ppm with a strength of 3.57 kHz. To decouple  $^{13}\text{C}$  from  $^2\text{H}$ , a decoupling field of 1.25 kHz strength at the  $^2\text{H}$  carrier frequency of

<sup>a</sup>Electronic mail: scshekar@medusa.bioc.aecom.yu.edu.

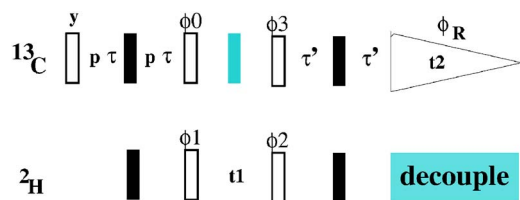


FIG. 1. (Color online) Pulse sequence for spin- $\frac{1}{2}$ -spin-1 pair HSQC, HDQC, coupled-HSQC, and coupled-HDQC experiments. All unmarked pulses are along the  $x$  axis. Open and filled boxes represent  $\pi/2$  and  $\pi$  pulses, respectively. The  $8j\tau=1$  and  $p=1,2$ , respectively, are for 1Q and 2Q experiments. For coupled experiments  $^{13}\text{C}$   $\pi$  pulse in the middle of the  $t_1$  period and  $^2\text{H}$  decoupling during  $t_2$  are turned off.  $\phi_R$  is the receiver phase. The phase cycling of the pulse and receiver phases ensures selection of the desired coherence transfer pathways and pure phase  $2d$  spectra with *in-phase* multiplets, in combination with proper choice of the  $\tau'=q\tau$  ( $q=0,1,2,\dots$ ) for each of the four experiments. See text for more details.

9.2 ppm was used. For all experiments a relaxation delay of 30 s was used. The spectral widths in all cases were 70 ppm along  $^{13}\text{C}$  and 12 ppm along  $^2\text{H}$ . In the  $2d$  experiments, the  $^{13}\text{C}$  signal was digitized with 1024 and 2048 complex (quadrature) time points for the uncoupled and coupled versions, respectively. The HSQC, coupled HSQC, HDQC, and coupled HDQC employed 16, 128, 16, and 56 complex increments in the indirect ( $^2\text{H}$ ) dimension, respectively. The corresponding experiments also employed 8, 16, 16, and 32 transients, respectively, for signal averaging. In all cases the  $2d$  data matrix was zero filled along  $t_2$  and  $t_1$  dimensions for a final size of 2048 and 128 complex points. Along both dimensions a cosine squared window function was applied prior to the Fourier transformation. A hypercomplex processing scheme was used to attain pure phase  $2d$  spectra<sup>7,15</sup> (see next section). All  $2d$  NMR data were processed in NMRPipe (Ref. 16) and converted to NMRView (Ref. 17) for viewing, analyzing, and generating postscript files to be included into TeX files (Ref. 18) to work in LaTeX (Ref. 19) environment.

### III. PULSE SEQUENCES

Figure 1 depicts the pulse sequences used to obtain HSQC, HDQC, coupled-HSQC, and coupled-HDQC correlation spectra. Quadrature detection is employed during acquisition. In the following, the identity

$$8J\tau=1 \quad (1)$$

is assumed. Kay and co-workers<sup>14</sup> have provided many details of the associated theory behind these experiments, and for most part only the expressions relevant to observable signals are presented here. For 1Q and 2Q experiments, respectively,

$$p=1,2. \quad (2)$$

$\tau'$  is selected appropriately as described later.

The phase cycling and the phase incrementation<sup>7,15,20</sup> (to attain phase sensitivity and pure phase) are as follows:

$$\phi'_0 = p - 1 + 2j, \quad j=0,1,$$

$$\phi'_1 = 1 + (2k + \xi)/p, \quad k=0,2p-1, \quad \xi=0,1,$$

$$\phi'_2 = 1 + 2l/p, \quad l=0,2p-1,$$

$$\phi'_3 = 1 - r + 2s, \quad r,s=0,1,$$

$$\phi'_R = 2(j+k-l-s) + r - 1, \quad (3)$$

where all phases have been expressed in units of  $\pi/2$ ,

$$\phi_k = \frac{\pi}{2}\phi'_k, \quad k=0,1,2,3,R. \quad (4)$$

$\xi=0,1$  represent the two components of the States scheme that are to be stored separately, subsequently engendering a double Fourier transform in a hypercomplex manner. States time proportional phase incrementation (TPPI) is achieved by appending an overall phase of  $\pi/p$  to  $\phi_1$  with each incrementation of the  $t_1$  value and taking this into account during processing.<sup>21</sup> The cycles  $l, s$  and step  $r=1$  may be dropped to keep phase tables relatively short.

For the coupled experiments, the  $^{13}\text{C}$   $\pi$  pulse in the middle of the  $t_1$  evolution period and  $^2\text{H}$  decoupling during  $t_2$  acquisition period are absent.

Below,

$$\theta' = 4\pi J\tau', \quad \theta_k = 2\pi Jt_k, \quad k=1,2. \quad (5)$$

#### A. HSQC

$$p=1 \text{ and } \tau'=\tau.$$

#### B. HDQC

$p=2$  and the signal is proportional to

$$f(\tau') = 1 - \cos \theta'. \quad (6)$$

In combination with the phase tables described above, using Eq. (1), the selection of

$$\tau' = q(2k+1)\tau, \quad q=1,2, \quad k=0,1,2,3,4,5, \dots, \quad (7)$$

ensures in-phase signal, with  $q=2$  yielding twice the signal as that of  $q=1$ . However,  $\tau'=4k\tau$  and  $k=0,1,2,3,4,5,\dots$ , lead to a null signal.

#### C. Coupled HSQC

$p=1$  and the signal is proportional to

$$f(t_1\tau't_2) = \cos\left(\frac{\theta_1}{2}\right) \sum_{m=1,0,-1} m e^{im(\theta'+\theta_2)}. \quad (8)$$

The resulting multiplet is a doublet separated by  $J$  along the indirect dimension. In the direct dimension, the central peak ( $m=0$ ) of the triplet will be missing, resulting in an *apparent* doublet separation of  $2J$ . Once again using Eq. (1), the hypercomplex procedure described above leads to pure phase spectra by setting the condition that

$$\tau' = k\tau \quad k=0,1,2,3, \dots \quad (9)$$

Now, the even multiples (including 0, i.e., abolishing the refocusing INEPT section altogether!) lead to an antiphase apparent doublet and the odd multiples lead to an in-phase apparent doublet.

## D. Coupled HDQC

Starting with equilibrium magnetization, the first  $y$  pulse in the sequence generates  $I$  spin ( $I=1/2, S=1$ )  $\pm 1$ QC's. The density matrix at the end of period  $4\tau$  is

$$\sigma(\tau) = I_x \{ 1 + [\cos(p4\pi J\tau) - 1] S_z^2 \} + \sin(p4\pi J\tau) I_y S_z. \quad (10)$$

With  $p=2$ , the  $I$ -spin  $\pi/2$  pulse with phase  $\phi_0$  in conjunction with the phase offset and cycling as specified by Eq. (4) is given by

$$-\sum_{\phi_0} e^{-i\phi_R} \sigma(\phi_0) = 2I_x \{ 1 + [\cos(8\pi J\tau) - 1] S_z^2 \}. \quad (11)$$

Imposing the condition of Eq. (1),

$$-\sum_{\phi_0} e^{-i\phi_R} \sigma(\phi_0) = 2I_x (1 - 2S_z^2). \quad (12)$$

$S$ -spin  $\pi/2$  pulse with phase  $\phi_1$  generates

$$\sigma(\phi_1) = \text{h.c.} + I_z (S_z^2 - 1 + S_z^2 e^{i2\phi_1}), \quad (13)$$

where "h.c." stands for "hermitian conjugate." Once again, imposing the phase conditions specified by Eq. (4) renders the density matrix into

$$\frac{1}{4} \sum_{\phi_1} e^{-i\phi_R} \sigma(\phi_1) = \text{h.c.} + I_z S_z^2 e^{i2\phi_1^0}, \quad \phi_1^0 = \frac{2\pi}{4}, \frac{3\pi}{4}, \quad (14)$$

where  $\phi_1^0$  denotes the "offset" of the phase  $\phi_1$  relative to which the phase cycling is carried out.

$$\sigma(t_1) = \text{h.c.} + e^{i2\phi_1^0} e^{i2\Omega_S t_1} I_z e^{i2\theta_1} I_z S_z^2, \quad (15)$$

where  $\Omega_S$  is the chemical shift of the  $S$  spin.

$$\sigma(\phi_2) = \text{h.c.} + e^{-i2\phi_2} e^{i2\phi_1^0} e^{i2\Omega_S t_1} I_z e^{i2\theta_1} I_z \left( 1 - \frac{3}{2} S_z^2 + A_s \right). \quad (16)$$

The term  $A_s$  exclusively comprises of  $S$ -spin operators.

$$A_s = \frac{1}{4} (\text{h.c.} + S_z^2 e^{i2\phi_2}) - \frac{i}{2} [S_z, \text{h.c.} + S_z e^{i\phi_2}]_+ \quad (17)$$

where the anticommutator is given by

$$[a, b]_+ = ab + ba. \quad (18)$$

The unobservable  $A_s$  may be dropped from  $\sigma(\phi_2)$  above, and in principle  $\phi_2$  phase cycling given by Eq. (4) may be omitted. Also, a three-step cycling would suffice as  $S_z S_\pm$  terms do not contribute to the signal. By dropping unobservable terms with  $I$ -spin operators, we have

$$\frac{1}{4} \sum_{\phi_2} e^{-i\phi_R} \sigma(\phi_2) = (\text{c.c.} + e^{i2\phi_1^0} e^{i2\Omega_S t_1}) \cos \theta_1 2I_x \times \left( 1 - \frac{3}{2} S_z^2 \right), \quad (19)$$

where "c.c." stands for "complex conjugate."

$$\sigma(\phi_3) = (\text{c.c.} + e^{i2\phi_1^0} e^{i2\Omega_S t_1}) \cos \theta_1 \{ \text{h.c.} + I_- e^{i(\phi_3 - \pi/2)} \} \times \left( 1 - \frac{3}{2} S_z^2 \right), \quad (20)$$

$$\frac{1}{2} \sum_{\phi_3} e^{-i\phi_R} \sigma(\phi_3) = (\text{c.c.} + e^{i2\phi_1^0} e^{i2\Omega_S t_1}) \cos \theta_1 2I_x \left( 1 - \frac{3}{2} S_z^2 \right). \quad (21)$$

At the end of subsequent period  $2\tau'$ ,

$$\sigma(\tau') = (\text{c.c.} + e^{i2\phi_1^0} e^{i2\Omega_S t_1}) \cos \theta_1 I_- e^{i\theta' S_z} \left( 1 - \frac{3}{2} S_z^2 \right), \quad (22)$$

where the unobservable  $I_+$  terms have been dropped.

$$\sigma(t_2) = (\text{c.c.} + e^{i2\phi_1^0} e^{i2\Omega_S t_1}) \cos \theta_1 e^{i\Omega_I t_2} I_- e^{i(\theta' + \theta_2) S_z} \times \left( 1 - \frac{3}{2} S_z^2 \right). \quad (23)$$

The signal in quadrature detection on  $I$ -spin channel then is given by<sup>7</sup>

$$F(t_1 \tau' t_2) = \sum_{m_I m_S} \langle m_I m_S | I_+ \sigma(t_1 \tau' t_2) | m_I m_S \rangle, \quad (24)$$

where  $m_I = \pm \frac{1}{2}$  and  $m_S \equiv m = 1, 0, -1$  are, respectively, the magnetic quantum numbers of spins  $I$  and  $S$ .

$$F(t_1 \tau' t_2) = (\text{c.c.} + e^{i2\phi_1^0} e^{i2\Omega_S t_1}) \cos \theta_1 e^{i\Omega_I t_2} \times \sum_{m=1,0,-1} \left( 1 - \frac{3}{2} m^2 \right) e^{im(\theta' + \theta_2)}. \quad (25)$$

Thus the signal, oscillating at a central frequency of  $2\Omega_S$  during  $t_1$  and  $\Omega_I$  during  $t_2$ , is proportional to

$$f(t_1 \tau' t_2) = \cos \theta_1 \sum_{m=1,0,-1} \left( 1 - \frac{3}{2} m^2 \right) e^{im(\theta' + \theta_2)}. \quad (26)$$

The multiplet now is a doublet with *doubled* separation ( $2J$ ), compared to the 1Q case, along the indirect dimension. In the direct dimension, the central peak ( $m=0$ ) of the triplet reappears with redoubled vigor (twice the intensity of the outer lines corresponding to  $m = \pm 1$ ), with an interpeak separation of  $J$ . Using Eq. (1) in Eq. (26), it is seen that only setting  $\tau'$  to even multiples of  $\tau$  (including dropping the refocusing INEPT part) yields pure phase spectra; odd multiples render outer lines out of phase (dispersive) with respect to the central line.

$$\tau' = 2k\tau, \quad k = 0, 1, 2, 3, \dots,$$

$$f(t_1 \tau' t_2) = \cos \theta_1 \left\{ 1 - \frac{1}{2} (-)^k (e^{i\theta_2} + e^{-i\theta_2}) \right\}. \quad (27)$$

Thus, only the odd values of  $k$  will lead to in-phase multiplets along the direct dimension, while the even values of  $k$  will result in the outer components being antiphase with respect to the central one.

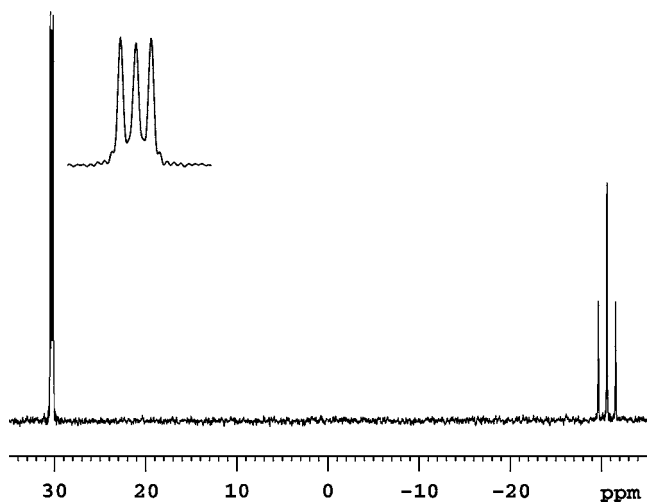


FIG. 2. Natural abundance  $^{13}\text{C}$  spectrum of 60%  $\text{C}_6\text{D}_6$  and 40% dioxane, with the carrier referenced to 0 ppm. The equidistant (25 Hz apart) triplet (1:1:1) centered at 30.3 ppm arises from the  $^{13}\text{C}$ - $^2\text{H}$  pair of  $\text{C}_6\text{D}_6$ , while the equidistant (142 Hz apart) triplet (1:2:1) centered at -30.6 ppm arises from the  $^{13}\text{C}$ - $^1\text{H}$  pair of dioxane. The  $\text{C}_6\text{D}_6$  multiplet is shown as an expansion in the inset next to the peak. See text for more details.

#### IV. RESULTS AND DISCUSSION

For the case here  $J \equiv J(^{13}\text{C}-^2\text{H}) = 25$  Hz.

In all figures, the  $^{13}\text{C}$  and  $^2\text{H}$  carriers have been referenced to 0 ppm.

Figure 2 shows the  $^{13}\text{C}$  spectrum of 60%  $\text{C}_6\text{D}_6$  and 40% dioxane. The contribution from  $\text{C}_6\text{D}_6$  is centered at 30.29 ppm, while that from dioxane is centered at

-30.6 ppm. The  $\text{C}_6\text{D}_6$  signal is a triplet of equal intensities and an interpeak separation equal to the  $^{13}\text{C}$ - $^2\text{H}$  indirect (scalar,  $J$ ) coupling. The triplet (with relative intensities of 1:2:1) due to dioxane has an interpeak separation of the  $^{13}\text{C}$ - $^1\text{H}$   $J$  coupling of 142 Hz. There are only two chemical shifts as all spins of a given nuclear species in both molecules are magnetically equivalent,<sup>22</sup> resulting in a single chemical shift for each nuclear species from a given molecule.

The panels of Fig. 3 show contour plots of the crosspeak bearing regions of the  $^{13}\text{C}$ - $^2\text{H}$  HSQC (left) and HDQC (right) correlation maps, respectively, obtained by setting  $\tau' = \tau$  (see previous section). The horizontal axis is the  $^{13}\text{C}$  frequency axis. The lone crosspeak is due to  $^{13}\text{C}$ - $^2\text{H}$  pairs from the  $\text{C}_6\text{D}_6$ , while the dioxane peaks have been edited out by the pulse sequence. The crosspeaks in the two contour plots show, along the  $^2\text{H}$  frequency axis, that the 2QC has double the precession frequency of the 1QC in the rotating frame rotating at the carrier frequency. Thus the right hand panel result is tantamount to doubling the magnetic field for the 1QC. For example, if the HSQC experiment was conducted at the as yet nonexistent hypothetical magnetic field strength corresponding to  $^1\text{H}$  Larmor frequency of 1200 MHz, the shift along  $^2\text{H}$  axis would be the same as in the right hand panel.

In Fig. 4, the regions bearing crosspeaks from the coupled-HSQC (left panel) and coupled-HDQC (right panel) spectra are shown. The condition  $8J\tau' = 1, 2$  was imposed, respectively, for the refocusing delays in the two experiments to obtain pure phase spectra and in-phase multiplets along

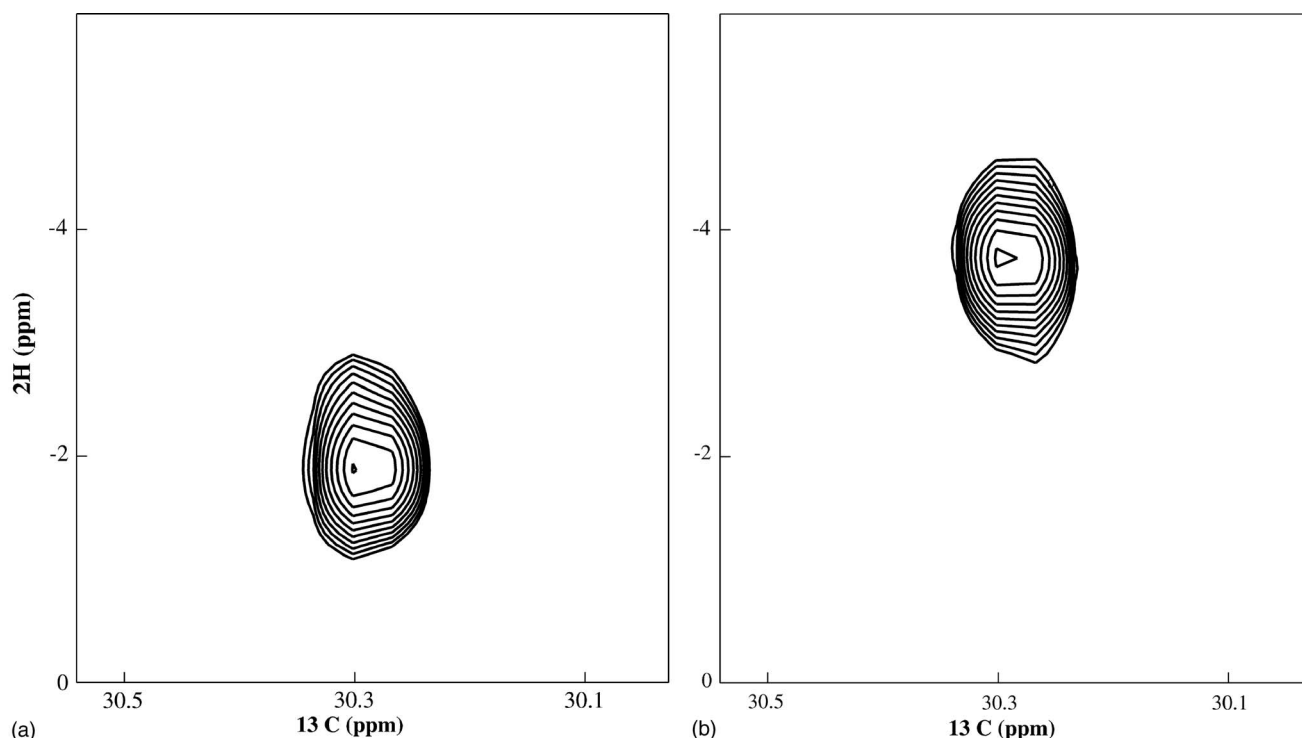


FIG. 3.  $^{13}\text{C}$ - $^2\text{H}$  correlation spectra of the same sample as in Fig. 2. The x axis is  $^{13}\text{C}$  chemical shift in ppm. The y axis is relative to the  $^2\text{H}$  carrier frequency of 9.2 ppm. Contour plots of the crosspeak bearing region of HSQC (left panel) and HDQC (right panel) spectra exhibit the frequency doubling of the 2QC coherence (along the  $^2\text{H}$  frequency axis) in the rotating frame rotating at the carrier frequency. The spectra were entirely bereft of the dioxane  $^{13}\text{C}$  peak at -30.6 ppm as it lacks any coupling to deuterons. The lone cross peak arises from the  $^{13}\text{C}$ - $^2\text{H}$  moiety, supplying the requisite spin- $\frac{1}{2}$ -spin-1 pair for successful observation of a correlation peak. See previous figures and text for more details.

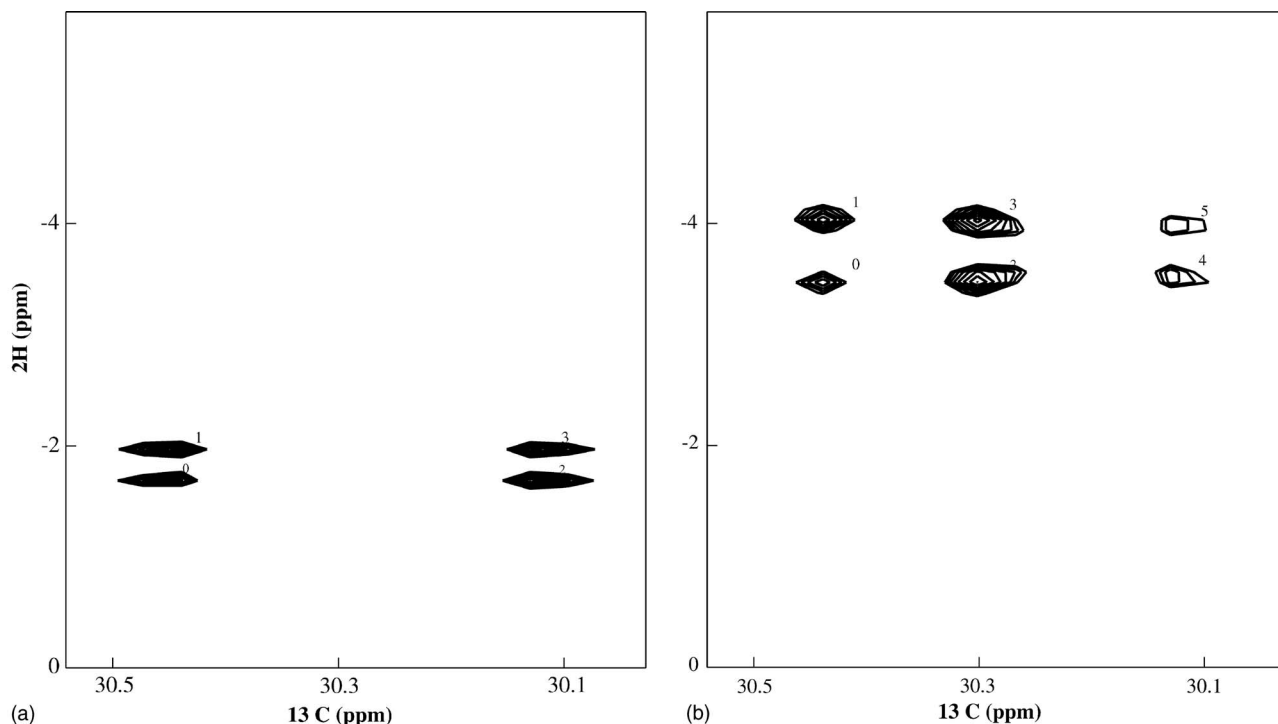


FIG. 4. Regions of coupled-HSQC (left panel) and coupled-HDQC (right panel) spectra containing crosspeak multiplets, exhibiting doubling of both the frequency and the coupling for the 2Q experiment along the 2Q axis. All crosspeaks are in phase. The condition  $8j\tau' = 1, 2$  was imposed, respectively, for 1Q and 2Q experiments. The coupled-HSQC pulse sequence yields a doublet along  $^2\text{H}$  (separated by  $J$ ) with equal weights. Along  $^{13}\text{C}$ , the central peak is conspicuously absent resulting in an *apparent* doublet of separation  $2J$ . The coupled-HDQC sequence again yields a doublet along the 2Q axis, but now with *twice* the separation ( $2J$ ). Along the 1Q axis a triplet with separation of  $J$  with the relative amplitudes of 1:2:1 is seen. See previous figures and text for more details.

the 1Q ( $^{13}\text{C}$ ) axis. These spectra exhibit the doubling of both the chemical shift and the coupling along  $^2\text{H}$  axis for the 2Q experiment. The coupled-HSQC pulse sequence yields a doublet along  $^2\text{H}$  (separated by  $J$ ) with equal weights. Along  $^{13}\text{C}$ , the intensities are proportional to  $m=1, 0, -1$ . The central peak is conspicuous by its absence and the resulting *apparent* doublet has a separation of  $2J$ . The coupled-HDQC sequence again yields a doublet along the 2Q axis, but now with *twice* the separation ( $2J$ ). Along the 1Q axis a triplet with separation of  $J$  with the relative amplitudes of 1:2:1 is seen. The implications of the formulas presented in the previous section for the multiplet patterns are borne out by these experiments. It should be noted that the coupling doubling exhibited in the coupled HDQC along the  $^2\text{H}$  dimension is solely a property of the 2Q coherence. In other words, unlike the shift frequency of the 1Q coherence, which can be doubled by doubling the magnetic field, the coupling experienced by 1Q coherence is not doubled. Furthermore, for both 1Q and 2Q coherences the coupling experienced and the resulting splitting are independent of the magnetic field strength.

Lastly, Fig. 5 graphs the ratio ( $R2Q1/R2Q2$ ) as a function of correlation time (characterizing the overall isotropic tumbling of a given molecule) in units of nanoseconds.  $R2Q1$  and  $R2Q2$  are, respectively, the contributions to the relaxation rates of 1Q and 2Q coherences associated with  $^2\text{H}$  due to the quadrupolar interaction as given by Millet *et al.*<sup>14</sup> In their notation  $R2Q1 \equiv R(D_+)$  and  $R2Q2 \equiv R(D_+^2)$ . We re-

produce the relevant formulas below, from the citation above, in a manner suitable for easy comparison and computation of the ratio;

$$R2Q1 = \frac{3}{80} \left[ \frac{e^2 q Q}{h/(2\pi)} \right]^2 [5J(\omega_D) + 2J(2\omega_D) + 3J(0)], \quad (28)$$

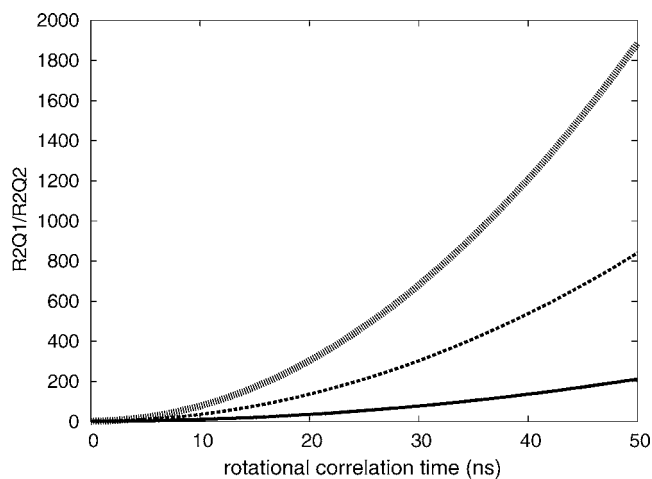


FIG. 5. Graphs of the ratio  $r=R2Q1/R2Q2$  as a function of correlation time (characterizing the overall isotropic tumbling of a given molecule) in units of nanoseconds.  $R2Q1$  and  $R2Q2$  are, respectively, the contributions to the relaxation rates of 1Q and 2Q coherences associated with  $^2\text{H}$  as given by Millet *et al.* (see text). The graphs are parametrized at three different magnetic field strengths corresponding to  $^1\text{H}$  Larmor frequencies of 300, 600 (the middle curve), and 900 MHz (thickest line).

$$R2Q2 = \frac{3}{80} \left[ \frac{e^2 q Q}{h/(2\pi)} \right]^2 [2J(\omega_D) + 4J(2\omega_D)], \quad (29)$$

from which it follows that

$$\frac{R2Q1}{R2Q2} = \frac{3J(0) + 5J(\omega_D) + 2J(2\omega_D)}{2J(\omega_D) + 4J(2\omega_D)}. \quad (30)$$

The symbols occurring on the right hand side of the three equations above have the same meaning as in the citation above.

The graphs are parametrized at three different magnetic field strengths corresponding to  $^1\text{H}$  Larmor frequencies of 300, 600, and 900 MHz. The calculations ignore any internal motion and show that the relaxation properties of 2Q coherence may be more favorable compared to that of 1Q coherence with increasing molecular weight and/or increasing field strength.

## V. CONCLUSIONS

Pulse sequences for spin- $\frac{1}{2}$ -spin-1 HSQC, HDQC, coupled HSQC, and coupled HDQC have been presented along with conditions for obtaining pure phase spectra with in-phase multiplet structure. Experimental demonstration on a  $^{13}\text{C}$ - $^2\text{H}$  bonded pair in solution state has been provided, exhibiting the frequency and coupling doubling in the 2Q experiments relative to the 1Q experiments, paving the way for possible resolution doubling in more complex systems with more than one spin- $\frac{1}{2}$ -spin-1 pair. In NMR, the resolution scales as the magnetic field strength. Thus the possibility to double the highly prized NMR resolution, that too without actually having to expend resources to physically double the magnetic field strength, is very inviting and further work seems warranted. It should also be noted that currently there are no (at least commercially) spectrometers available equipped with magnets whose strengths correspond to  $^1\text{H}$  Larmor frequencies greater than 900 MHz (which would be seen by the 2Q coherence as 1800 MHz magnet for  $^1\text{H}$ !). Furthermore, whatever the magnetic field is, the 2Q coherence would behave as if the field strength was double the actual one.

## ACKNOWLEDGMENTS

This work was supported by NIH under Grant Nos. GM55692 (J.M.B.) and GM072085(M.E.G.), and by a Mentor-Based Fellowship from the American Diabetes Association (S.C.S.). S.C.S is grateful to Professor Vern L. Schramm for inspiration.

- <sup>1</sup>Z. Gan, *J. Am. Chem. Soc.* **128**, 6040 (2006).
- <sup>2</sup>S. Cavadini, A. Lupulescu, S. Antonijevic, and G. Bodenhausen, *J. Am. Chem. Soc.* **128**, 7706 (2006).
- <sup>3</sup>S. Cavadini, S. Antonijevic, A. Lupulescu, and G. Bodenhausen, *J. Magn. Reson.* **182**, 168 (2006).
- <sup>4</sup>L. Mueller, *J. Am. Chem. Soc.* **101**, 4481 (1979).
- <sup>5</sup>G. A. Morris and R. Freeman, *J. Am. Chem. Soc.* **101**, 760 (1979).
- <sup>6</sup>G. Bodenhausen and D. J. Ruben, *Chem. Phys. Lett.* **69**, 185 (1980).
- <sup>7</sup>R. R. Ernst, G. Bodenhausen, and A. Wokaun, *Principle of Nuclear Magnetic Resonance in One and Two Dimensions* (Clarendon, Oxford, 1987).
- <sup>8</sup>J. Cavannah, W. J. Fairbrother, A. G. Palmer III, and N. J. Skelton, *Protein NMR Spectroscopy* (Academic, New York, 1996), Chap. 7, p. 412.
- <sup>9</sup>C. A. Fyfe, K. C. Wong-Moon, Y. Huang, and H. Grondey, *J. Am. Chem. Soc.* **117**, 10397 (1995).
- <sup>10</sup>C. A. Fyfe, H. M. zu Altschildesche, K. C. Wong-Moon, H. Grondey, and J. M. Chezeau, *Solid State Nucl. Magn. Reson.* **9**, 97 (1997).
- <sup>11</sup>H. Kao and C. P. Grey, *J. Magn. Reson.* **133**, 313 (1998).
- <sup>12</sup>D. Massiot, F. Fayon, B. Alonso, J. Trebosc, and J. Amoureux, *J. Magn. Reson.* **164**, 160 (2003).
- <sup>13</sup>D. R. Muhandiram, T. Yamazaki, B. D. Sykes, and L. E. Kay, *J. Am. Chem. Soc.* **117**, 11536 (1995).
- <sup>14</sup>O. Millet, D. R. Muhandiram, N. R. Skrynnikov, and L. E. Kay, *J. Am. Chem. Soc.* **124**, 6439 (2002).
- <sup>15</sup>D. J. States, R. A. Haberkorn, and D. J. Ruben, *J. Magn. Reson.* (1969-1992) **48**, 286 (1982).
- <sup>16</sup>F. Delaglio, S. Grzesiek, G. W. Vuister, G. Zhu, J. Pfeifer, and A. Bax, *J. Biomol. NMR* **6**, 277 (1995).
- <sup>17</sup>B. A. Johnson and R. A. Blevins, *J. Biomol. NMR* **4**, 603 (1994).
- <sup>18</sup>D. E. Knuth, *The TeXbook* (Addison-Wesley, Reading, Massachusetts, 1984).
- <sup>19</sup>L. Lamport, *LaTeX: A Document Preparation System* (Addison-Wesley, Reading, Massachusetts, 1986).
- <sup>20</sup>A. Wokaun and R. R. Ernst, *Chem. Phys. Lett.* **52**, 407 (1977).
- <sup>21</sup>D. Marion, M. Ikura, R. Tschudin, and A. Bax, *J. Magn. Reson.* (1969-1992) **85**, 393 (1989).
- <sup>22</sup>H. S. Gutowsky, D. W. McCall, and C. P. Slichter, *J. Chem. Phys.* **21**, 279 (1953).